PHYSICAL REVIEW C VOLUME 23, NUMBER 4 APRIL 1981

# Nuclear structure of $^{26}$Al studied by two-nucleon transfer reactions $^{28}$Si($d,\alpha$) and $^{24}$Mg($^3$He,$p$)

N. Takahashi,* Y. Hashimoto, Y. Iwasaki,† K. Sakurai,‡ F. Soga,§ K. Sagara,‖ and Y. Yano¶
*Department of Physics, Faculty of Science, University of Tokyo, Bunkyo-ku, Tokyo, Japan*

M. Sekiguchi
*Institute for Nuclear Study, University of Tokyo, Tanashi-shi, Tokyo, Japan*

(Received 25 August 1980)

The differential cross sections for the reactions $^{28}$Si($d,\alpha$)$^{26}$Al and $^{24}$Mg($^3$He,$p$)$^{26}$Al were measured at the incident energies of 33.0 and 27.5 MeV, respectively, in order to investigate the structure of $^{26}$Al in connection with the nuclei $^{28}$Si and $^{24}$Mg. The angular distributions and the relative magnitudes of the cross sections were analyzed by using the distorted-wave Born approximation theory of the two-nucleon transfer reactions. The shapes of the calculated angular distributions reproduced well the experimental data. The transferred angular momenta $L$ extracted from the angular distributions were consistent with the spins and parities already known. A qualitative picture of the structure of the nucleus $^{26}$Al from the data of the relative transition strengths of the two-nucleon transfer reactions was attempted using two simple models of nuclear structure, the Nilsson model with pairing correlations and the simple pairing model of a spherical nucleus. In the former the final state was described by a single configuration of two Nilsson quasiparticles and in the latter, by a single configuration of two quasiparticles in a spherical basis. This Nilsson model showed that the two-nucleon transfer strengths for the low-lying states of $^{26}$Al supported the idea that there exist states with opposite signs of the deformation parameter in the low-lying states of $^{26}$Al. The simple pairing model predicted well the overall features of the two-nucleon transfer strengths. This success evolved from the assumption that the final states of $^{26}$Al were described separately for stripping to $^{24}$Mg and pickup from $^{28}$Si by using realistic values of the occupation number probabilities for the shell model orbitals of the respective nuclei. These facts suggest also the existence of states with different character in the $^{26}$Al nucleus.

[NUCLEAR REACTIONS $^{28}$Si($d,\alpha$)$^{26}$Al, $E_d$=33.0 MeV and $^{24}$Mg($^3$He,$p$)$^{26}$Al, $E_{^3\mathrm{He}}$=27.5 MeV; measured $\sigma(E_\alpha,\theta)$ and $\sigma(E_p,\theta)$; enriched $^{28}$Si and $^{24}$Mg targets. DWBA analysis, deduced $L$, $J^\pi$. Analysis with Nilsson model with pairing correlation and simple pairing model of spherical nucleus.]

## I. INTRODUCTION

The nucleus $^{26}$Al is located in the transition region between prolate and oblate shapes, making it difficult to obtain a unified description of its involved level structure. Experimentally, the level scheme of $^{26}$Al below 5 MeV is well known.[1] The spin and parities of these levels were determined mainly by $\beta$- and $\gamma$-decay studies.[2-13] In these studies, the lifetimes of these levels and the electromagnetic transition strengths between them were also measured. Spectroscopic data on $^{26}$Al have also been obtained by means of such particle transfer reactions as ($^3$He, $d$),[14,15] ($d,n$),[16] ($^3$He, $p$),[17-19] ($\alpha, d$),[19,20] ($p,d$),[21,22] ($^3$He, $\alpha$),[23] and ($d,\alpha$).[24,25]

No single model of the nuclear structure has been successful in describing all of the observed spectroscopic properties. Horvat *et al.*[3] successfully interpreted the low-lying states observed in the ($p,\gamma$) experiment with a simple Nilsson model with a prolate deformation. This model, however, was found to be inadequate in explaining both the single-particle spectroscopic factors deduced from the various single-nucleon transfer reactions,[14-16,21,23] and the data from the two-nucleon transfer reactions.[17] The rotational model with extensive band mixing via the Coriolis coupling[26] gave a good explanation of the level density but did not adequately account for the electromagnetic properties. A shell-model calculation[22] with the truncated basis space of the $1s$-$0d$ shell qualitatively reproduced the energy spectrum and agreed better with the observed single-neutron pickup strengths[21,22] than the simple Nilsson model did. On the other hand, Sharpey-Schafer *et al.*[9] and Price *et al.*[10] presented evidence for the rotational bands by observing high-spin states and their $\gamma$-ray transitions. This fact indicates that $^{26}$Al can be a deformed nucleus.

All of these preceding results may reflect the versatile character of this nucleus. Recently, Brut and Jang[27] pointed out the importance of the multiplicity of Hartree-Fock intrinsic states with different shapes for the nuclei in the transition region between the prolate and oblate deformations, such as for the nuclei of $^{27}$Al and $^{27}$Si. Thus, the nuclear structure of $^{26}$Al may be characterized by the existence of various intrinsic states with different natures.

While a detailed high-resolution study of the two-nucleon stripping reaction $^{24}$Mg($^3$He, $p$)$^{26}$Al (Ref. 17) was made at the incident energy of 18 MeV, information about the two-nucleon pickup reac-

 

tion[24,25] is very limited. Therefore, we performed an experiment on the $^{28}$Si$(d, \alpha)^{26}$Al reaction at 33 MeV. An emphasis was placed on a high energy resolution to obtain clear separations of many states involved, up to 5 MeV in excitation, and a systematic measurement of their angular distributions. In addition, the reaction $^{24}$Mg$(^3$He$, p)^{26}$Al was repeated at a higher incident energy, 27.5 MeV, to obtain a set of data for spectroscopic analysis from both the stripping and pickup reactions. We are particularly interested in analyzing the relative intensity of the cross sections for the transfers to various final states. These intensities were analyzed by two different nuclear models, the Nilsson model with pairing correlation and the simple pairing model of a spherical nucleus. In the former, each final state of $^{26}$Al is described by a single configuration of two Nilsson quasiparticles. In the latter, each final state is described by a single configuration of two quasiparticles on a spherical basis. The present analyses of the cross sections using these two different models produce a qualitative picture for the nuclear structure of $^{26}$Al, which can be characterized by the existence of various intrinsic states with different deformations.

Section II gives the experimental procedures and results. The methods of analysis are described in Sec. III. Results calculated by the distorted-wave Born approximation (DWBA) are compared with the experimental data in Sec. IV, and a discussion and conclusions are presented in Sec. V.

## II. EXPERIMENTAL PROCEDURES AND RESULTS

### A. $^{28}$Si$(d,\alpha)^{26}$Al reaction

An analyzed beam of 33.0-MeV deuterons was obtained from the INS-SF cyclotron (a sector-focusing cyclotron) at the Institute for Nuclear Study, University of Tokyo (INS).[28] Its energy spread was estimated to be less than 10 keV.[29] The target was a $^{28}$Si self-supporting foil prepared by the vacuum evaporation of enriched $SiO_2$ powder (99.84%) with Ta reduction. The thickness was estimated to be 67 $\mu$g/cm$^2$.[30]

Alpha particles from reactions were analyzed with a quadrupole-dipole-dipole- (QDD-) type magnetic spectrograph.[31] The solid angle of the spectrograph was 1.93 msr. A 40-cm single-wire gas proportional counter[32] with resistive readout was used as the position-sensitive detector along the focal plane. This length covered an energy range of about 4 MeV for the detected $\alpha$ particles. Its position was adjusted to minimize the kinematic energy spread. Two additional gas proportional counters backed up the position counter and were used to suppress the background yields in the measured spectra. Alpha-particle spectra were measured at 12 laboratory angles between $\theta_L = 6°$ and 60°. The energies of the $\alpha$ particles were calibrated with known peaks from the contaminants $^{12}$C and $^{16}$O and those from the $^{26}$Si$(d, \alpha)$ reaction to known states of the final nucleus.

A typical spectrum measured at 12° laboratory angle is shown in Fig. 1. The overall energy resolution was about 30 keV at full width half maximum (FWHM). Alpha-particle groups from contaminants $^{12}$C and $^{16}$O masked peaks of interest above 3.5 MeV in excitation energy at some angles. This spectrum of the $\alpha$ particle covers the excitation energy region of up to 9 MeV in $^{26}$Al. Twenty-four peaks were identified below 5 MeV as coming from the $^{28}$Si$(d, \alpha)^{26}$Al reaction. The correspondence between their excitation energies and those of the known levels[1] is given in Table I. Errors in the excitation energies are estimated to be 6 keV. No peak above 5 MeV had enough intensity to attract our interest.

Angular distributions were obtained for twenty-three $\alpha$ groups, and are shown in Fig. 2. Some points in the angular distributions are missing because of the contamination. The errors shown in the figures are from the counting statistics and background subtraction. The uncertainty in the absolute values of the cross sections was estimated to be 20%.

### B. $^{24}$Mg$(^3$He$,p)^{26}$Al reaction

This experiment was made by using the INS FF cyclotron (an ordinary cyclotron) facility at INS.[33] An analyzed beam of 27.5-MeV $^3$He from the cyclotron was used to bombard a $^{24}$Mg target. The target was prepared by the vacuum evaporation of enriched MgO (99.96%) with Ti reduction onto a gold backing. The thickness was estimated[34] to be 0.34 mg/cm$^2$ in $^{24}$Mg.

The protons from the reaction were analyzed with a magnetic spectrograph and were recorded on nuclear emulsion plates 2.5 cm wide, 25 cm long, and 100 $\mu$m thick placed along the focal plane. An aluminum absorber 400 $\mu$m thick was used in front of the plates to stop all particles except the protons. One exposure covered an energy range of about 10 MeV. The solid angle was typically 0.3 msr. The proton energies were calibrated by using peaks corresponding to known low-lying states in $^{26}$Al.

A typical spectrum measured at 10° laboratory angle is shown in Fig. 3. The overall energy resolution was about 60 keV at FWHM. This resolution resulted mainly from the beam-energy spread, resolution of the spectrograph, and target

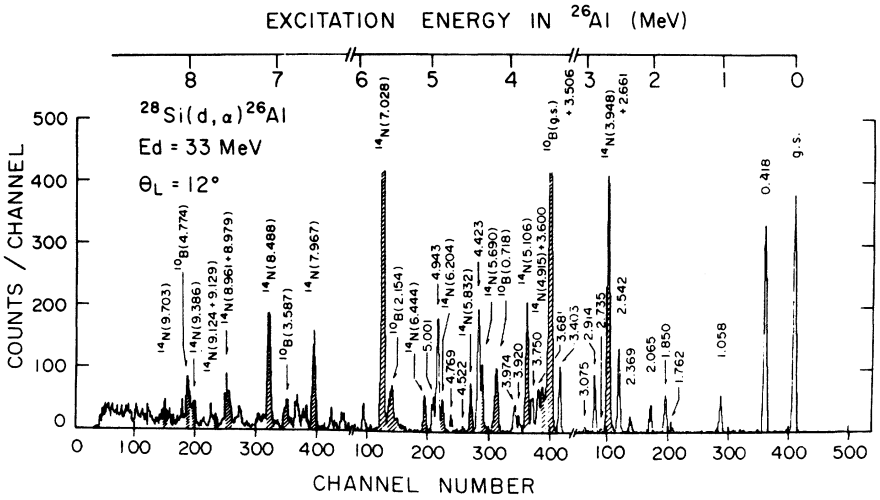


FIG. 1. Alpha-particle spectrum from the $^{28}$Si$(d,\alpha)^{26}$Al reaction measured at 33.0 MeV incident energy and at a laboratory angle of 12°. Alpha-particle groups from the $^{28}$Si$(d,\alpha)^{26}$Al reaction are denoted by the excitation energies of the residual nucleus in MeV. Those from the contaminants are hatched and labeled by the residual nuclei and their excitation energies.

thickness. Proton groups from the contaminants $^{12}$C and $^{16}$O were not found, except for those for a few low-lying states of the respective final nuclei. Many strongly populated peaks were observed at high excitation energies and were identified to come from the $^{24}$Mg$(^3$He$,p)^{26}$Al reaction. Possible errors in the excitation energies were estimated to be 20 keV below 6 MeV in excitation and 30 keV above it. The excitation energies for the observed groups and those of the known levels are given in Table I.

Angular distributions of the proton groups corresponding to the isolated low-lying states and the strongly populated states in a higher excitation-energy region are given in Figs. 4 and 5. The errors from counting statistics and background subtraction are shown in those figures. The uncertainty in the absolute cross sections is about 20%.

## III. METHOD OF ANALYSIS OF CROSS-SECTION DATA

The differential cross section for a direct two-nucleon transfer reaction $A(a,b)B$ can be written as the following by assuming zero-range interaction and neglecting spin-orbit potentials both in the incident and outgoing channels[35-37]

$$\left(\frac{d\sigma}{d\Omega}\right)_{\mathrm{DW}} \propto \sum_{LST} C_{ST}^{\,2} \left| \sum_{\alpha_1\alpha_2} S^{1/2}(\alpha_1\,\alpha_2; JT) \begin{pmatrix} l_1 & l_2 & L \\ \frac{1}{2} & \frac{1}{2} & S \\ j_1 & j_2 & J \end{pmatrix} B_{\Lambda}^{L}(\theta, E, Q) \right|^2 . \tag{1}$$

In this expression, the symbols $L$, $S$, $J$, and $T$ are orbital, spin, total angular momentum, and isospin carried by the transferred pair, respectively, and $\alpha \equiv (n, l, j, m, m_t)$ describes a single-nucleon orbit. The coefficient $C_{ST}$ contains the Clebsch-Gordan coefficient for the isospins, the spectroscopic factors for the light particles $a$ and $b$, and the strength factor of the spin-isospin exchange terms in the interaction potential. The factor ( ) is the $jj$- to $LS$-coupling transformation coefficient. These two factors, $C_{ST}$ and ( ), give the selection rules for the angular momentum and isospin. The factor $S^{1/2}(\alpha_1\,\alpha_2; JT)$ is the spectroscopic amplitude for the two-particle configuration $(\alpha_1\,\alpha_2)_{JT}$. This is essentially the parentage factor which connects the nucleus $B$ with the nucleus $A$, and depends on the nuclear-structure model used. The factor $B_{\Lambda}^{L}(\theta, E, Q)$ is the usual distorted-wave amplitude.

The angular distributions are analyzed by the DWBA primarily to deduce the transferred $L$ value and, hence, the spins and parities of the final states of $^{26}$Al. The magnitudes of the cross sections calculated by assumed nuclear models are compared with those observed to get more information on the nuclear structure of $^{26}$Al. We are particularly interested in analyzing the relative intensity of the cross sections for the transitions

TABLE I. Energy levels of $^{26}$Al. The results of previous works and those of the present study by means of the $^{28}$Si$(d,\alpha)^{26}$Al and $^{24}$Mg$(^3$He$,p)^{26}$Al reactions are compared. $\sigma^{max}(\theta)$ is the differential cross section at the maximum of the angular distribution.

| Previous works [a] | | | Present study | | | | | | |
|---|---|---|---|---|---|---|---|---|---|
| | | | $^{28}$Si$(d,\alpha)^{26}$Al | | | $^{24}$Mg$(^3$He$,p)^{26}$Al | | | |
| Excitation energy (MeV) | $J^\pi$ | $T$ | Excitation energy (MeV) | $\sigma^{max}(\theta)$ ($\mu$b/sr) | $L$ | Excitation energy (MeV) | $\sigma^{max}(\theta)$ ($\mu$b/sr) | $L$ | Assignment [b] $J^\pi$ |
| 0.0 | $5^+$ | | 0.0 | 1440 | 4 | 0.0 | 51 | 4 | |
| 0.228 | $0^+$ | 1 | 0.23 | 7 [d] | | 0.23 | 147 | 0 | |
| 0.417 | $3^+$ | | 0.418 | 893 | 2 | 0.42 | 277 | 2 | |
| 1.058 | $1^+$ | | 1.058 | 108 | 0+2 | 1.05 | 125 | 0+2 | |
| 1.759 | $2^+$ | | 1.762 | 11 | 2 | 1.76 | 10 [e] | | |
| 1.850 | $1^+$ | | 1.850 | 96 | 0+2 | 1.85 | 441 | 0+2 | |
| 2.069 | $4^+$ | | | | | | | | |
| 2.070 | $2^+$ | 1 | 2.065 | 46 | 4 | 2.07 | 120 | | |
| 2.072 | $1^+$ | | | | | | | | |
| 2.365 | $3^+$ | | 2.369 | 28 | 4 | 2.36 | 95 | 2+4 | |
| 2.545 | $3^+$ | | 2.542 | 147 | 2+(4) | 2.55 | 81 | 2 | |
| 2.661 | $2^+$ | | 2.661 | 8 | 2 | 2.66 | 20 | 2 | |
| 2.739 | $1^+$ | | 2.735 | 9 | 0+2 | 2.74 | 35 | 2 | |
| 2.913 | $2^+$ | | 2.914 | 90 | 2 | 2.91 | 29 | 2 | |
| 3.073 | $3^+$ | | 3.075 | 9 | 2+(4) | 3.07 | 60 | 4 | |
| 3.160 | $2^+$ | 1 | | | | 3.16 | 137 | 2 | |
| 3.403 | $5^+$ | | 3.403 | 170 | 4 | 3.40 | 10 [e] | | |
| 3.508 | $6^+$ | | 3.506 | 30 | 6 | | | | |
| 3.595 | $3^+$ | | 3.600 | 70 | 2 | 3.59 | 68 | (2) | |
| 3.674 | $4^+$ | | | | | | | | |
| 3.681 | $3^+$ | | 3.681 | 113 | 2 | | | | |
| 3.723 | $1^+$ | | | | | | | | |
| 3.750 | $(2,3)^+$ | | 3.750 | 94 | 2 | 3.75 | 226 | | |
| 3.753 | $0^+$ | 1 | | | | | | | |
| 3.923 | $7^+,(5)^+$ | | 3.920 | 34 | | | | | $(5)^+$ |
| 3.963 | $3^+$ | | 3.974 | 75 | 1 | | | | $(0^-,1^-)$ |
| 3.979 | $(0,1)$ [c] | | | | | | | | |
| 4.191 | $3^+$ | (1) | | | | | | | |
| 4.205 | $4^+$ | | | | | | | | |
| 4.349 | $(1,3)^+$ | | | | | 4.35 | 135 | (0)+2 | |
| 4.430 | $2^-$ | | 4.423 | 342 | 1 | | | | $(1,2)^-$ |
| 4.479 | $\pi$ = unnatural | | | | | | | | |
| 4.547 | $(2,3)^+$ | (1) | | | | 4.55 | 160 | | |
| 4.599 | $3^+$ | (1) | | | | 4.61 | 290 | | |
| 4.622 | $(1^+,2^-,3^+)$ | | | | | | | | |
| 4.705 | $(3,4)^+$ | 1 | | | | | | | |
| 4.772 | $(3,4)^+$ | | 4.769 | 34 | 4 | | | | |
| 4.938 | $1^-$ | | | | | | | | |
| 4.952 | $3^+$ | | 4.943 | 330 | 2+4 | | | | |
| 5.006 | $(0-5)^+$ | | 5.001 | 83 | | | | | |
| | | | | | | 5.87 | 490 | | |
| | | | | | | 6.27 | 250 | | |
| | | | | | | 6.42 | 335 | | |
| | | | | | | 6.59 | 275 | | |
| | | | | | | 6.72 | 470 | | |
| | | | | | | 6.87 | 350 | | |
| | | | | | | 7.11 | 190 | | |
| | | | | | | 7.40 | 580 | | |
| | | | | | | 7.81 | 340 | | |
| | | | | | | 8.04 | 330 | | |
| | | | | | | 9.29 | 490 | | |
| | | | | | | 10.07 | 395 | | |

[a] Taken from Ref. 1.
[b] See the text for assignment.
[c] Taken from Refs. 8 and 12.
[d] Value at $\theta_L = 15°$.
[e] Values at $\theta_L = 15°$.

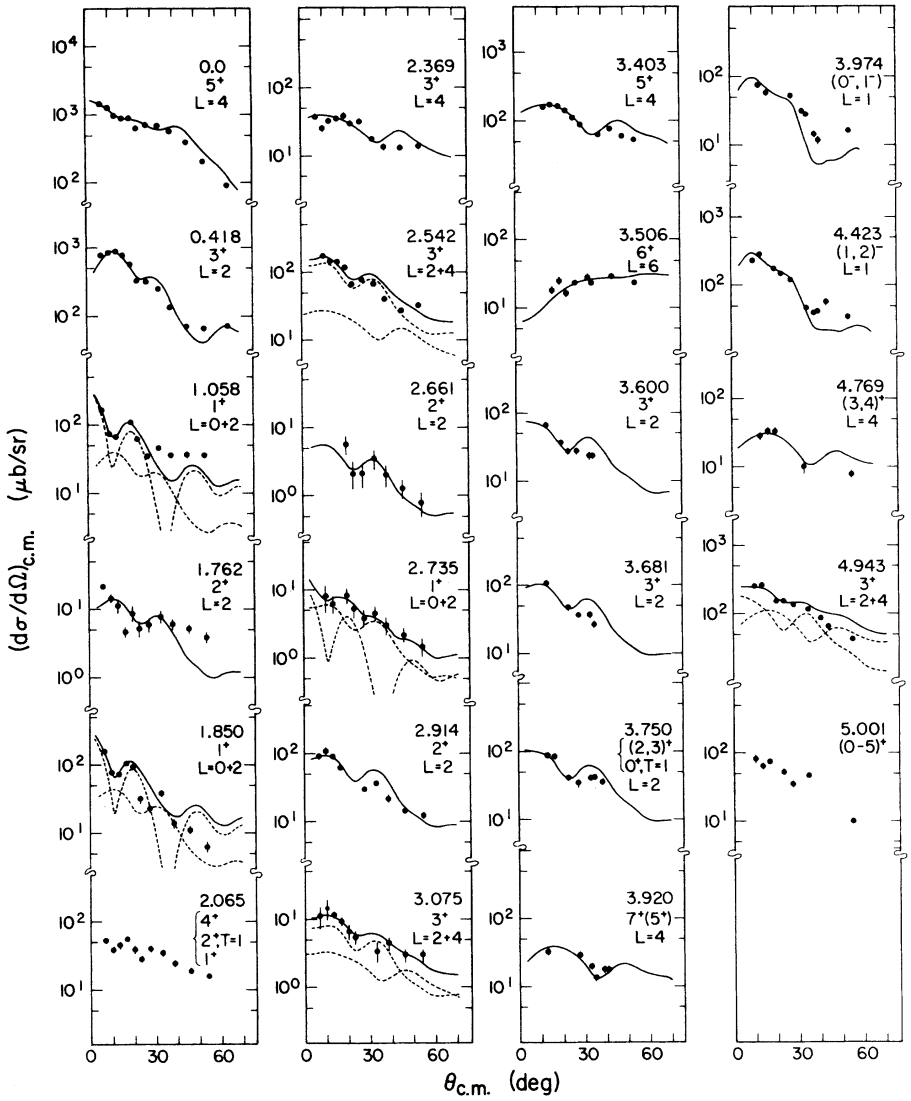


FIG. 2. Angular distributions of the $^{28}$Si$(d,\alpha)^{26}$Al reaction measured at 33.0 MeV bombarding energy. They are labeled by the excitation energies in MeV and $J^\pi$ values of the final states and the transferred $L$ values. The $J^\pi$ values in the bracket are the possible candidates for that level. The solid curves are the results of the DWBA calculations using the optical parameters in Table III. The calculated curves were adjusted by the eye to fit the experimental data. The dashed curves represent the components of the cross section when two $L$ values contribute to the reaction. The triplet at 2.065 MeV excitation energy was not resolved and the summed yields are shown. The level at 3.750 MeV is an unresolved doublet. The 3.974-MeV level is not resolved from the 3.963-MeV $3^+$ level, but the yield of the latter seems to be small (see text).

to various final states.

As mentioned in Sec. I, the $^{26}$Al nucleus is located in the transition region between the prolate and oblate shapes, and is so complicated that no single model has been known to describe all of its spectroscopic properties quantitatively. Gamma-ray studies[9,10] produced evidence for the two rotational bands in $^{26}$Al, while the single nucleon pcikup strengths to low-lying states[21,22] were predicted better by the detailed shell-model calculations than by the simple Nilsson model. Recently, the importance of the interplay between the prolate and oblate shapes was shown for the nuclei of $^{27}$Al and $^{27}$Si in the transition region.[27] Therefore, the nuclear structure of $^{26}$Al may have the multiple character of various intrinsic states with different natures.

In this analysis, we adopt two different simple modles, the Nilsson model with pairing correlation and the simple pairing model of spherical

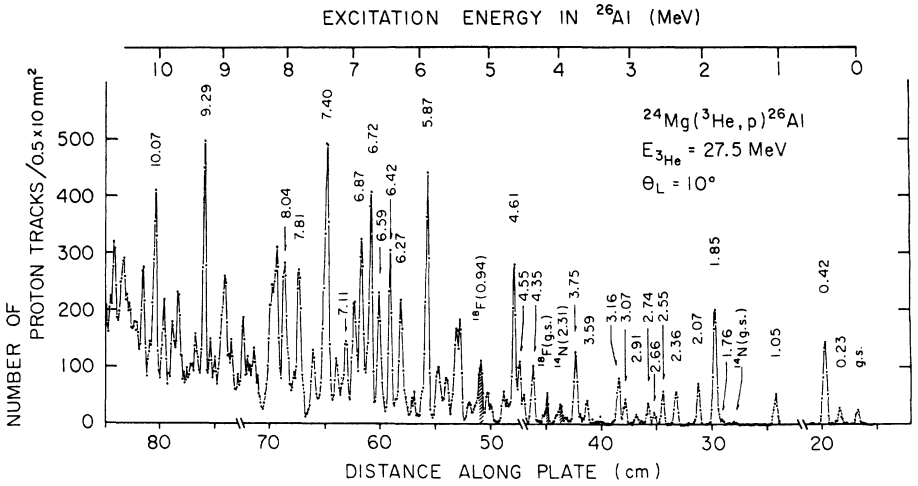


FIG. 3. Proton spectrum from the $^{24}$Mg($^{3}$He,$p$)$^{26}$Al reaction measured at 27.5 MeV incident energy and at a laboratory angle of 10°. Proton peaks from this reaction are designated by the excitation energies of the residual nucleus $^{26}$Al in units of MeV. Identified impurity peaks are hatched and labeled by the final nuclei and their excitation energies.

nucleus, and attempt to produce a qualitative picture for the nuclear structure of $^{26}$Al, rather than to determine which model is better. This picture of $^{26}$Al can be characterized by the existence of various intrinsic states with different natures.

### A. Theoretical two-nucleon spectroscopic amplitudes

#### *1. Model 1: Nilsson model with pairing correlation*

The general formalism for calculating two-nucleon spectroscopic amplitudes with the Nilsson

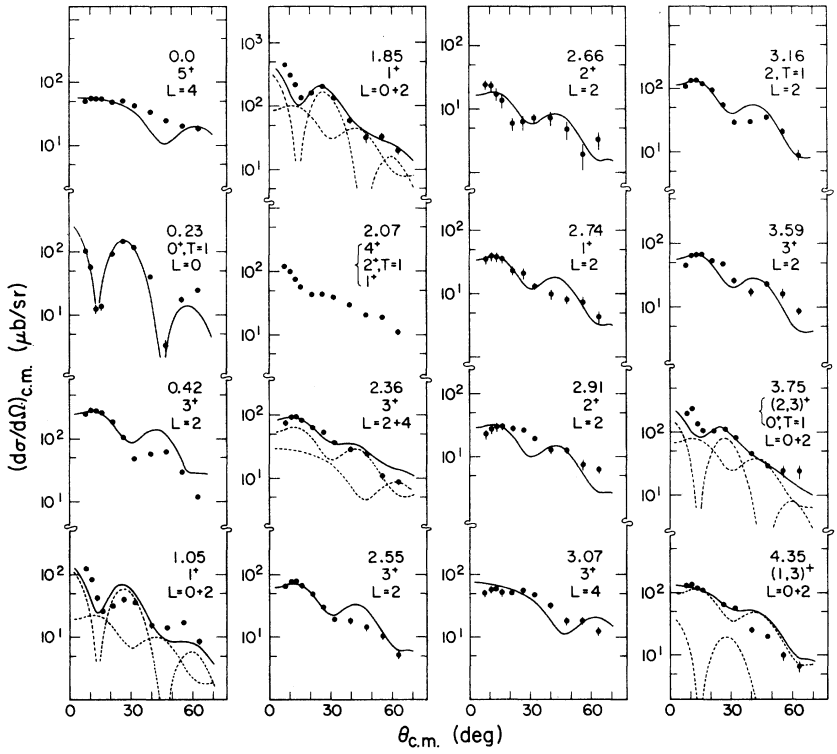


FIG. 4. Angular distributions of the $^{24}$Mg($^{3}$He,$p$)$^{26}$Al reaction at a bombarding energy of 27.5 MeV. See Fig. 2 for the notations. The level at 2.07 MeV is an unresolved triplet, and the level at 3.75 MeV is an unresolved doublet.

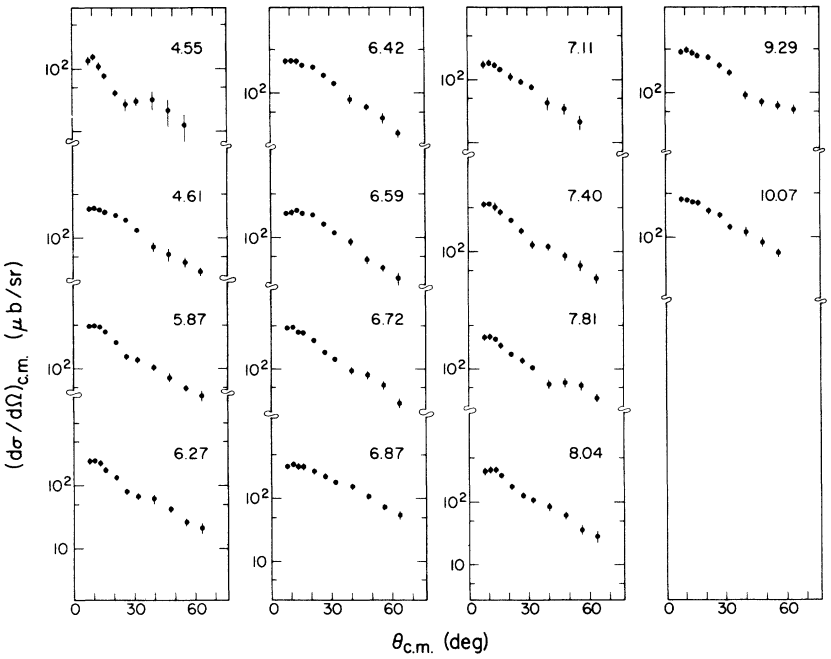


FIG. 5. Angular distributions of the proton peaks located in the higher excitation-energy region of $^{26}$Al and populated strongly by the $^{24}$Mg($^3$He,$p$)$^{26}$Al reaction. The angular distributions are labeled by the excitation energies (MeV) in $^{26}$Al.

model with pairing correlation is discussed in Ref. 38. Here we present only the basic assumptions and resulting equations which were required for the present analysis of the ($d$, $\alpha$) and ($^3$He, $p$) reactions.

One assumes the rotational wave functions of the adiabatic form[39] for the initial and final states. The intrinsic particle motion is assumed to be described by the Nilsson model with pairing correlation. However, this model neglects the interaction between proton and neutron quasiparticles as well as the Coriolis coupling. The ground states of the even-even nuclei, $^{24}$Mg and $^{28}$Si, are the BCS vacuum of the Nilsson quasiparticles. An intrinsic excited state of $^{26}$Al, as well as the ground state, is constructed by exciting two quasiparticles (one proton and one neutron) from the BCS vacuum.

If the difference between initial and final BCS vacuums is neglected, the spectroscopic amplitudes in Eq. (1) are given by

$$S^{1/2}(I_i = K_i = 0, \alpha_1 \alpha_2, J;\ I_f = J, K_f, T_f) = U_{\gamma_1} U_{\gamma_2} S_0^{1/2} \tag{2}$$

for the stripping to $^{24}$Mg, and

$$S^{1/2}(I_i = K_i = 0,\ \alpha_1 \alpha_2, J;\ I_f = J, K_f, T_f) = -(2J+1)^{1/2} V_{\gamma_1} V_{\gamma_2} S_0^{1/2} \tag{3}$$

for the pickup from $^{28}$Si, where $U_\gamma(V_\gamma)$ is a probability amplitude for the Nilsson state $\gamma$ to be empty (full). In the above expressions, $S_0^{1/2}$ is the spectroscopic amplitude in the simple Nilsson model,[40] i.e.,

$$S_0^{1/2} = \left(\frac{2}{(2I+1)(1+\delta_{K_f,0})}\right)^{1/2} \{(j_1\omega_1 j_2\omega_2 | I_f K_f) W^{\gamma_1}_{j_1\omega_1} W^{\gamma_2}_{j_2\omega_2} + (-)^{T_f}(j_1\omega_2 j_2\omega_1 | I_f K_f) W^{\gamma_2}_{j_1\omega_2} W^{\gamma_1}_{j_2\omega_1}\}, \tag{4}$$

where $W^\gamma_\alpha$ is the transformation coefficient between the shell-model single-particle orbital $\alpha$ and the Nilsson single-particle orbital $\gamma$. The probability amplitudes $U_\gamma$ and $V_\gamma$ of the Nilsson single-particle states were calculated by the usual BCS method.[41] The Nilsson single-particle states arising from the $0d_{5/2}$, $1s_{1/2}$, and $0d_{3/2}$ shell-model states were taken into account in constructing the BCS vacuum. The wave functions of these Nilsson states were generated in a deformed oscillator-potential well with a quadrupole deformation. They were expanded in the spherical states originating from the same major harmonic-oscillator shell. The parameters of the Nilsson single-particle Hamiltonian[42] adopted were $\omega_0 = 41.2/A^{1/3}$ MeV, $\kappa = 0.0878$, and $\mu = 0.0218$. These values of $\kappa$ and $\mu$ were chosen so as to reproduce the single-particle energies of 0.0, 2.57, and 6.03 MeV (Ref. 43) for the shell-model states of $0d_{5/2}$, $1s_{1/2}$, and $0d_{3/2}$, respectively. The strength

of the pairing was adjusted for a given deformation parameter $\beta$ to give a gap of about 2.33 MeV, the average odd-even mass difference in the mass region concerned. The values of the strength thus obtained ranged between $26.6/A$ and $36.6/A$ MeV for the range of $-0.3 \leq \beta \leq 0.3$ in the cases of $^{24}$Mg and $^{28}$Si nuclei.

*2. Model 2: simple pairing model of spherical nucleus*

In the simple pairing model of a spherical nucleus, it is assumed that each final state of $^{26}$Al is described by a single configuration of two quasiparticles of a proton and a neutron on spherical basis. This implies that such a pair of particles (holes) is formed by adding (removing) a $(j_\pi j_\nu)_J$ proton-neutron pair to (from) the target. The spectroscopic amplitudes in this model are given by the quasiparticle expression[35,36]

$$S^{1/2}(j_\pi j_\nu; J) = U_{j_\pi} U_{j_\nu} \tag{5}$$

for ($^3$He, $p$), and

$$S^{1/2}(j_\pi j_\nu; J) = -(2J+1)^{1/2} V_{j_\pi} V_{j_\nu} \tag{6}$$

for ($d$, $\alpha$), where $U_j(V_j)$ is a probability amplitude for the shell model orbital $j$ to be emtpy (full), and $\pi$ and $\nu$ stand for proton and neutron, respectively. These probability amplitudes are calculated with the occupation numbers of proton and neutron, $n_\pi$ and $n_\nu$, for the orbitals $j_\pi$ and $j_\nu$ in the target nucleus, respectively. The occupation numbers adopted for the $^{24}$Mg and $^{28}$Si ground states are taken from experimental data[44] and from a shell-model calculation,[43] respectively. They are listed in Table II. In the present calculations, we assumed that $n_{j_\pi} = n_{j_\nu}$.

B. DWBA calculations

DWBA calculations were performed with the zero-range approximation and without the spin-orbit coupling by using the two-nucleon transfer option of the code TWOSTP.[45] The two-particle form factor was evaluated according to the Bayman and Kallio method.[46] The single-particle wave function of the transferred proton or neutron was calculated by using a real potential of Woods-Saxon form. The depth of the potential well was chosen so as to reproduce the single-nucleon separation energy, which was taken as

$\frac{1}{2}$(deuteron separation energy + 2.225 MeV).

The Gaussian shape was used for the interaction potential between the transferred particles and the relevant incident and outgoing particles. The depth and size parameters of the potential were $V_0 = 62.2$ MeV and $\beta^2 = 0.379$ fm$^{-2}$.[47] The Gaussian wave functions were assumed for the light particles. The size parameters used were $\eta_d = 0.163$ fm$^{-1}$, $\eta_\alpha = 0.233$ fm$^{-1}$, and $\eta_{^3\mathrm{He}} = 0.207$ fm$^{-1}$ in the Glendenning notation[36] for the deuteron, $\alpha$ particle, and $^3$He particle, respectively.

Calculations with the sets of potential parameters available in the literature[48] could not reproduce the experimental angular distributions of the present $^{28}$Si($d$,$\alpha$)$^{26}$Al reaction. Therefore, we searched for the optical-model parameters to fit elastic cross sections by using the code ELAST II[49] under the condition of "well-matching criterion."[50] In these searches, the radius and diffuseness parameters of the real wells were fixed at the physically reasonable values of $r_R = 1.25$ and $a = 0.75$ fm, respectively. The angular distributions for the ($d$, $\alpha$) reaction were calculated with those parameters thus obtained for the deuteron and $\alpha$ particle. The imaginary-well depth of the deuteron potential was further changed a little to improve the fit of the calculations to the experimental data. In the case of the ($^3$He, $p$) reaction, the experimental angular distributions were fitted by the use of the optical-model parameters in Ref. 51 for $^3$He and the proton. However, the real-well depth of the proton potential was modified to give a better fit to these experimental data. Table III lists the sets of optical-potential parameters used.

Angular distributions were calculated for various two-particle configurations formed from the pairs of the shell-model orbitals 0$p$, 0$d$, 1$s$, 0$f$, 1$p$, and 0$g$. Shapes of the calculated angular distributions for single-$L$ transfer were found to be insensitive to the two-particle configurations belonging to the same major shell. Therefore, the following configurations were adopted for $L$-value assignments: $(0d_{5/2})^2$ for even $L(\leq 4)$, $(0d_{5/2}0g_{9/2})$ for $L = 6$, and $(0d_{5/2}0p_{1/2})$ for odd $L$.

The calculated DWBA cross sections were multiplied by a factor $N$ to produce the theoretical cross sections which were compared with the experimental data:

$$\left(\frac{d\sigma}{d\Omega}\right)_{\mathrm{theor}} = N \left(\frac{d\sigma}{d\Omega}\right)_{\mathrm{DW}}. \tag{7}$$

The factor $N$ was determined for each reaction

TABLE II. Occupation numbers of the shell-model orbitals for the protons and neutrons in $^{24}$Mg and $^{28}$Si, used in the calculations of the spectroscopic amplitudes in the case of model 2. Numbers of protons and neutrons ($n_\pi$ and $n_\nu$) are assumed to be the same.

| Nucleus | $n_\pi = n_\nu$ $0d_{5/2}$ | $1s_{1/2}$ | $0d_{3/2}$ | Reference |
|---|---|---|---|---|
| $^{24}$Mg | 3.00 | 0.30 | 0.70 | 44 |
| $^{28}$Si | 5.05 | 0.65 | 0.30 | 43 |

TABLE III. Optical-potential parameters used in the DWBA calculations for the $^{24}$Mg($^3$He, $p$)$^{26}$Al reaction at an incident energy of 27.5 MeV and for the $^{28}$Si($d,\alpha$)$^{26}$Al reaction at 33.0 MeV. In the calculations, the spin-orbit potentials in all channels were neglected. The optical potential has the form

$$U(r)=U_C-Vf(x_R)-i\left(W-4a_I w_0\frac{d}{dx_I}\right)f(x_I),$$

where $f(x)=(1+e^x)^{-1}$, $x_i=(r-r_i A^{1/3})/a_i$, and $U_C$ is the Coulomb potential with a radius parameter $r_C$.

| Channel | $V$ (MeV) | $W$ (MeV) | $W_D$ (MeV) | $r_R$ (fm) | $a_R$ (fm) | $r_I$ (fm) | $a_I$ (fm) | $r_C$ (fm) |
|---|---|---|---|---|---|---|---|---|
| $^3$He | 173.9 | 20.6 | | 1.15 | 0.72 | 1.50 | 0.82 | 1.40 |
| $p$ | 50.0 | | 13.0 | 1.20 | 0.70 | 1.25 | 0.70 | 1.25 |
| $d$ | 78.4 | | 15.0 | 1.25 | 0.75 | 1.34 | 0.68 | 1.25 |
| $\alpha$ | 199.4 | 11.3 | | 1.25 | 0.75 | 1.65 | 0.64 | 1.25 |

by normalizing the DWBA cross section calculated with model 2 to the experimental one for the transition to the ground state. The ground state is believed to have an almost pure configuration $(d_{5/2})^2$ and model 2 employs the realistic value of the occupation number of this configuration for each target ground state (see Sec. III A 2). The values of $N$ used are 273 for the $(d,\alpha)$ reaction and 10.5 for the $(^3\mathrm{He},p)$ reaction. The value $N$ required for the former reaction might possibly be the result of our using the "well-matching condition."[50]

## IV. CALCULATED RESULTS AND COMPARISON WITH EXPERIMENT

### A. Angular distributions

The angular distributions calculated by the DWBA are shown with the respective experimental data in Fig. 2 for the $(d,\alpha)$ reaction and in Fig. 4 for the $(^3\mathrm{He},p)$ reaction. The calculated curves were adjusted by the eye to give the best fit to the data. According to the selection rules[37] for the reaction concerned, the angular distributions leading to natural-parity states have shapes characteristic of single-$L$-value transfers. In the case of unnatural-parity states, the cross sections are incoherent sums of those for two values of $L$. In the present analysis, the relative strength at these two transfers were determined to reproduce the experimental angular distributions. (Examples can be seen in the transition to the 1.850 MeV $1^+$ state, etc.) Most of the levels of $^{26}$Al below 5 MeV in excitation have well known spins, parities, and isospins.[1] The ground $5^+$ state is believed to have a dominant $(d_{5/2})^2_{J=5}$ configuration for which $L=6$ is forbidden. The transition to this state, therefore, is expected to be an almost pure $L=4$ transfer. The calculated $L=4$ shape reproduced well the experimental $(d,\alpha)$ angular distribution. The $(^3\mathrm{He},p)$ shape for an $L=4$ transfer also showed an acceptable fit to the experimental data. The calculated shape for the 3.403-MeV state gave a good fit to the observed shape with $L=4$ only in the case of the $(d,\alpha)$ reaction, although the shape was considerably different from that for the ground state. This is a typical example in which the DWBA calculation could reproduce different shapes of the angular distributions with the same $L$ but different $Q$ values.

Any transition to the $J^\pi=0^+$ state is forbidden for the present $(d,\alpha)$ reaction, whereas the observed angular distributions for the 1.058- and 1.850-MeV $1^+$ states were fitted well by the dominated $L=0$ DWBA curves. The transition to the $2^+$ $T=0$ states at 1.762 and 2.914 MeV were candidates for the pure $L=2$ shape. The observed angular distributions for these $2^+$ states were fitted fairly well by the calculations. In the $(^3\mathrm{He},p)$ reaction, the transitions to the 0.228-MeV $0^+$ $T=1$ state and the 3.160-MeV $2^+$ $T=1$ state are allowed. The calculated angular distributions for the $L=0$ and $L=2$ shapes reproduced well the observed shapes for these states. The angular distribution to the 3.506-MeV state, the only known $6^+$ state, was obtained in the $(d,\alpha)$ reaction, and this was fitted well by a calculated $L=6$ shape with a configuration $(d_{5/2}g_{9/2})_6$.

Thus in summary, the calculated angular distributions reproduced well those of experiments for cases of the single-$L$-value transfers and also for cases of incoherent sums of the cross sections for two values of $L$. The present results for the transferred $L$ values extracted from the angular distributions were consistent with the spins and parities already known,[1] except for those discussed below.

The following comments are applicable to some levels of $^{26}$Al.

*The 3.920-MeV level.* Price *et al.*[10] assigned $J=7^+$ to this state, although they did not exclude the possibility of $5^+$. The $^{27}$Al$(p,d)$ experiment of Show *et al.*[22] suggested $l_n=4$ for the transition to this state. Although the data points are quite limited, our $(d,\alpha)$ angular distribution seemed to prefer the $L=4$ transfer to the $L=6$ one, which leads to a possible assignment of $5^+$. We could not exclude, however, the possibility of a close doublet of $5^+$ and $7^+$ states at this energy.

*The 3.974-MeV level.* Our 3.974-MeV level was likely to be the 3.979-MeV state observed in high-resolution studies of the $(^3\text{He},p\gamma)$ reaction[8] and the $(p,d)$ reaction.[22] Its spin was suggested to be 0 or 1 by the $^{24}$Mg$(^3\text{He},p\gamma)$ works.[7,8] This level was not resolved from the 3.963-MeV level in our $(d,\alpha)$ reaction, but its angular distribution showed a dominant $L=1$ shape. This suggested that the transition to the 3.963-MeV $3^+$ state was weak and that the 3.979-MeV state had the spin-parity of $0^-$ or $1^-$.

*The 4.423-MeV level.* The spin-parity of this level was shown to be $(1\text{-}4)^-$ by the $(^3\text{He},\alpha)$ reaction on $^{27}$Al (Ref. 23) and $(1\text{-}4)^-$ by the $(p,d)$ reaction.[22] This state was strongly populated via the present $(d,\alpha)$ reaction, and its angular distribution was reproduced well by the $L=1$ DWBA curve. These results showed the spin-parity of this state to be $1^-$ or $2^-$, which is consistent with a recent compilation.[1]

The preceding information on the transferred $L$ values, spins, and parities are listed in Table I, together with the maximum values of the cross sections for both reactions.

### B. Relative transition strengths

#### *1. Model 1: Nilsson model with pairing correlation*

The Nilsson model without configuration mixing has been applied to the low-lying states of $^{26}$Al.[14-17,21,23] In this simple Nilsson model, the intrinsic states are formed by two particles, a proton and a neutron, outside a prolate $^{24}$Mg core. The ground $5^+$ and 3.506-MeV $6^+$ states have been identified as the two lowest members of a $K=5$ band[9] formed by coupling two nucleons in Nilsson orbital $\frac{5}{2}[202]$. The 0.228-MeV $0^+$, 1.058-MeV $1^+$, and 2.070-MeV $2^+$ states are members of $K=0$ $(T=0,1)$ bands which result from the antiparallel coupling of the particles in the same orbital. The 0.418-MeV $3^+$, 2.069-MeV $4^+$, and 3.403-MeV $5^+$ states have been assigned as the three members of a $K=3$ band[10] formed on an intrinsic state of a parallel coupling of a $\frac{5}{2}[202]$ particle to a $\frac{1}{2}[211]$ one. The 1.762-MeV $2^+$ state is assigned to be the lowest member of a $K=2$ band[3] built on the antiparallel coupling of these two particles.

In the simple Nilsson model with a sharp boundary of the Fermi surface, the $\frac{5}{2}[202]$ orbital is full of protons and neutrons in the ground state of $^{28}$Si, while the $\frac{1}{2}[211]$ orbital is empty. Hence, the transitions to the states with configurations such as $(\frac{5}{2}[202]\times\frac{1}{2}[211])$ should be largely hindered in the $^{28}$Si$(d,\alpha)$ reaction. The transitions to such states are found in our data of the $^{28}$Si$(d,\alpha)$ reaction. The 0.418-MeV $3^+$ and 3.403-MeV $5^+$ states are populated with considerable yields which suggest that the Fermi surface is diffused in the Nilsson model, as was observed also in the $(t,\alpha)$ reactions on $^{24}$Mg and $^{28}$Si.[44] Recently, the influence of pairing on a particle-rotor model description of the $1s$-$0d$ shell nucleus, $^{23}$Na, has been investigated,[52] and most of the available experimental data could be described well within the framework of this model.

In the present analysis, the Nilsson model with pairing interaction is used. The Fermi surface is diffused in this model. In Figs. 6 and 7, the diagrams of the calculated single-particle energies of the Nilsson-particle and Nilsson-quasiparticle orbitals are shown. The configurations of the Nilsson quasiparticles were assumed to be the same as those described in the previous paragraphs on the simple Nilsson model. In

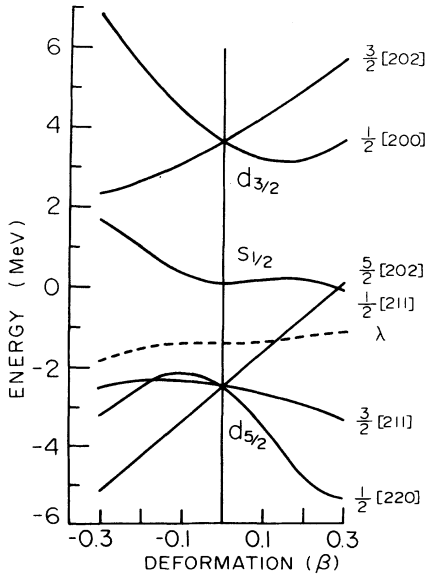


FIG. 6. Energy levels of the Nilsson orbitals as a function of the deformation parameter $\beta$ in the case of $^{26}$Al. The parameters in the Nilsson single-particle Hamiltonian adopted in the calculation were $\omega_0=41.2/A^{1/3}$, $\kappa=0.0878$, and $\mu=0.0218$. The dashed curve indicates the Fermi level in $^{26}$Al.

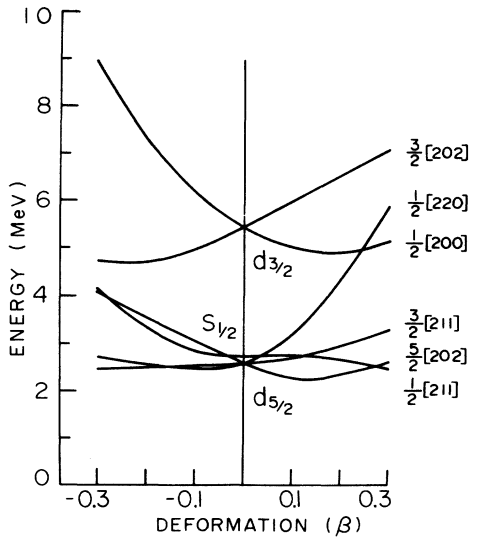


FIG. 7. Energy levels of the Nilsson-quasiparticle orbitals as a function of the deformation parameter $\beta$ in the case of $^{26}$Al. The strength of the pairing force was adjusted for each value of the deformation parameter to give a gap of 2.33 MeV. This value of the gap is equal to the average odd-even mass difference in the region of mass number 26.

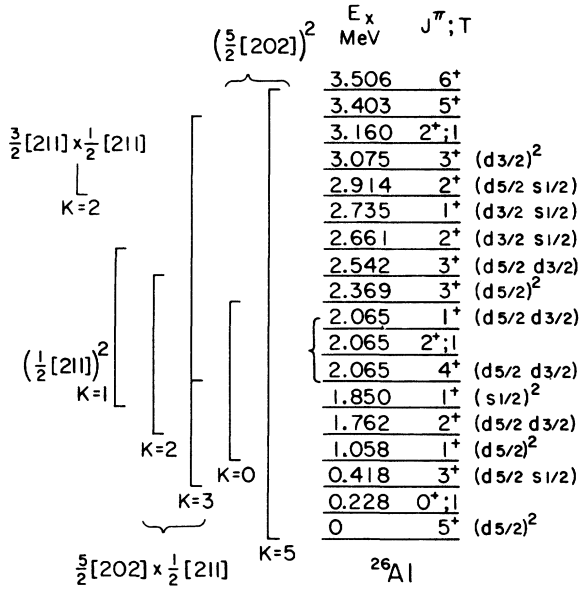


FIG. 8. Bands and their configurations of two Nilsson quasiparticles in the Nilsson model with pairing correlation (model 1) and configurations of two quasiparticles in the simple pairing model of the spherical nucleus (model 2), assumed in the DWBA calculations for the low-lying states of $^{26}$Al. Model 1 describes the final states in $^{26}$Al as single configurations of the two Nilsson quasiparticles, shown at the left of the figure. In model 2, these states are described by single configurations of two quasiparticles on a spherical basis, shown at the right of the figure. See the text for further details on the calculations.

addition, the 2.368-MeV $3^+$ and the 2.542-MeV $3^+$ states were assumed to be members of the $K=0$ band with a configuration of $(\frac{5}{2}[202])^2$ and the $K=2$ band with a $(\frac{5}{2}[202]\times\frac{1}{2}[211])$, configuration, respectively.[53] The 1.850-MeV $1^+$ and 2.661-MeV $2^+$ states were assumed to be the members of a $(\frac{1}{2}[211])^2$ band with $K=1$, instead of $K=0$,[17] and the 2.914-MeV state to be $(\frac{3}{2}[211]\times\frac{1}{2}[211])_{K=2}$. The bands and their configurations assumed for the low-lying states of $^{26}$Al are shown in Fig. 8. It should be noted that the present analysis was limited to the $T=0$ states in $^{26}$Al because of comparison between the $(d,\alpha)$ and $(^3\mathrm{He},p)$ reactions.

Figure 9 shows a comparison between the observed cross sections and the calculated ones for the assumed configurations in a range of the deformation parameter $-0.3\leq\beta\leq 0.3$. In the calculated results, the same deformation $\beta$ was assumed for the initial and final nuclei. The calculated cross sections are normalized to the experimental ones for the ground $5^+$ state for both reactions, as was described in Sec. III B. In the case of the $^{24}$Mg$(^3\mathrm{He},p)$ reaction, the relative values calculated with a prolate deformation around $\beta=0.2-0.3$ agreed fairly well with the observed strengths for the $K=1$, $K=2$, and $K=3$ bands. As for the 2.065-MeV $4^+$ state, the experimental cross section shown in Fig. 9 is that for the unresolved triplet which includes the other two states ($2^+$, $T=1$, and $1^+$), and this may yield the experimental cross section larger than the prediction. The predicted values for the $K=5$ and $K=0$ bands deviate largely from the experimental ones. In the case of the $(d,\alpha)$ reaction, the strengths for the $K=5$ and $K=0$ bands predicted with an oblate deformation reproduce well the experimental data, although such is not the case for the other bands. The results of the $(d,\alpha)$ reaction are opposite to those of the $(^3\mathrm{He},p)$ reaction.

The relative values of the calculated transition strengths of various states within the $K=5$ and $K=0$ bands of the same configuration $(\frac{5}{2}[202])^2$ are independent of $\beta$, as is seen in the results presented in Fig. 9. This is due to the fact that the Nilsson orbital $\frac{5}{2}[202]$ contains only one shell-model orbital $d_{5/2}$. The ratios of the calculated maximum cross section of the ground $5^+$ state to the 1.058-MeV $1^+$ state is 10.5 for the $(^3\mathrm{He},p)$ reaction, and it is 13.2 for the $(d,\alpha)$ reaction, irrespective of $\beta$. The ratios measured experimentally are 0.41 for $(^3\mathrm{He},p)$ and 13.3 for $(d,\alpha)$. The calculation disagrees with the experiment in the ratio for the $(^3\mathrm{He},p)$ reaction, but agrees well with that for the $(d,\alpha)$ reactions.

It should be noted that most of the angular distributions considered are insensitive to variation

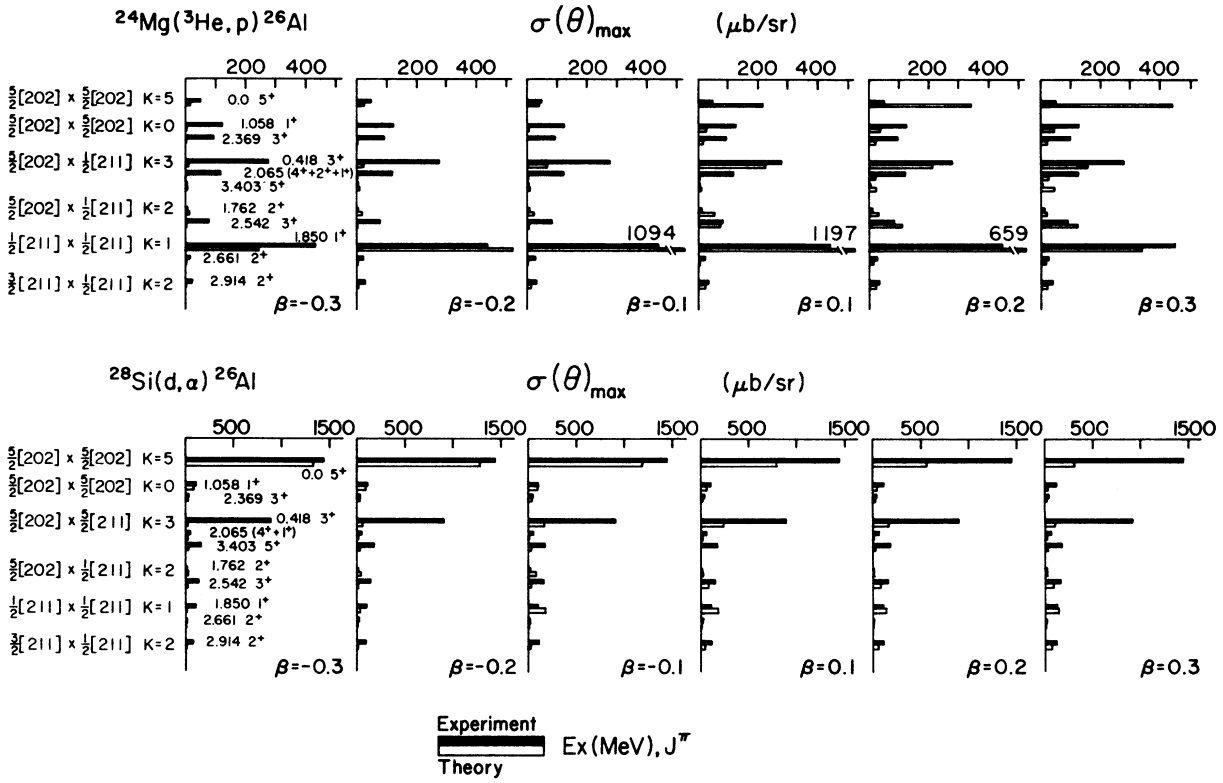


FIG. 9. Comparison of the theoretical cross sections (model 1) with the experimental ones in the $^{24}$Mg($^3$He, $p$) and $^{28}$Si($d$, $\alpha$) reactions for each value of the deformation parameter $\beta$. The lengths of the bars represent the maximum differential cross sections in units of μb/sr. The solid and open bars are for the experimental and theoretical cross sections, respectively. The theoretical cross sections were obtained by normalizing the calculationed ones, as described in Sec. III.

in the values of $\beta$ since the angular distributions for the natural parity states, which are produced by single $L$ transfer, are little changed by the two-particle configuration mixing that consisted of the same major shell-model orbitals. Also, the unnatural parity states with the $(\frac{5}{2}[202])^2$ configuration only contain the $(d_{5/2})^2$ configuration. This leaves only three states, i.e., 0.418-MeV $3^+$, 1.850-MeV $1^+$, and 2.543 MeV $3^+$, which could be used to test this model by such a $\beta$ dependence. The results indicate a preference that $\beta$ be 0.2–0.3.

The above results may be explained as follows. In the framework of the present model, the difference of deformation between the initial and final nuclei is not taken into account explicitly; the core overlap of the initial and final states is assumed to be unity. In fact, $^{24}$Mg is prolate and $^{28}$Si is oblate.[54] It is reasonable, therefore, to assume that the overlap of the cores is unity for the final states with $\beta > 0$ in the case of the ($^3$He, $p$) reaction and unity for those with $\beta < 0$ in the case of the ($d$, $\alpha$) reaction. The results obtained here from the comparison between the theory and experiment may suggest that the $K = 0$ and $K = 5$ bands have the opposite sign of the deformation parameter to the other bands.

The following points should be noted. The present model does not take into account the residual interaction between proton and neutron quasiparticles and the Coriolis coupling. The configurations adopted in the present calculations were simple, and further detailed comparison between theory and experiment may not be well-founded. In the case of the ground state, however, the configuration can be believed to be pure in the frame of the $1s$-$0d$ shell.[14-16,21-23] The overestimation of the transition strength for the ground state in the case of the ($^3$He, $p$) reaction could be reduced if the core overlap were properly taken into account.

### 2. *Model 2: simple pairing model of spherical nucleus*

In the present analysis, each final state of this $^{26}$Al nucleus is described by a single, two-quasiparticle configuration of a spherical basis. In

other words, the final states of $^{26}$Al are produced by adding (removing) a single pair of particles to (from) the target ground state. The configuration for each level in this model was assumed by taking a dominant component of the shell model basis in the two-Nilsson-quasiparticle configuration in model 1. In addition, these configurations for the final states are not inconsistent with the experimental spectroscopic data obtained from single nucleon transfer reactions.[14-16,21-23]

Figure 10 shows the comparison between the calculated and observed cross sections for the $^{24}$Mg($^3$He, $p$) and $^{28}$Si($d$, $\alpha$) reactions. The calculated cross sections were normalized to those for the ground $5^+$ state in both reactions, as was described in Sec. III B. Disagreements between the predictions and the experimental results can be seen for the 2.369-, 2.542-, and 3.075-MeV $3^+$ states, and the 2.661-MeV $2^+$ state. The transitions to those states associated with a $0d_{3/2}$ orbital are much weaker than the predicted ones, especially for the ($^3$He, $p$) reaction. The difficulty with this model may be caused by the fact that it puts the $0d_{3/2}$ orbital much too low in excitation energy in $^{26}$Al. It should be emphasized, however, that the predicted values reproduced well the general features of the experimental data for both reactions, despite the simplicity of the model. The prediction explains especially well the experimental ratios of the cross sections between the transitions to the ground $5^+$ and the

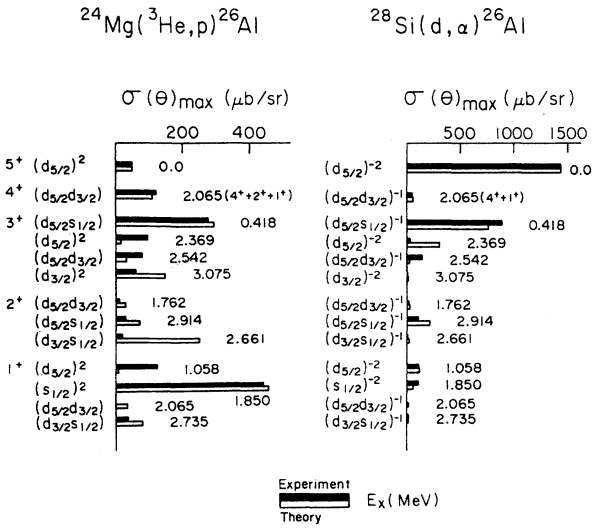


FIG. 10. Comparison of the theoretical cross sections (model 2) with the experimental ones for the $^{24}$Mg($^3$He, $p$) and $^{28}$Si($d$, $\alpha$) reactions. The diagram should be read as described in the caption of Fig. 9. The theoretical cross sections were obtained by normalizing the calculated cross sections to the experimental ones for the ground-state transitions.

1.850-MeV $1^+$ states for both reactions. The angular distributions are also in general agreement between the prediction and the experiment.

These results show that our assumption underlying the reaction mechanism is valid in the present ($^3$He, $p$) and ($d$, $\alpha$) reactions, in which the reactions proceed by adding (removing) two nucleons to (from) the target ground state without disturbing it, and that the present simple model for the final states of $^{26}$Al is adequate for explaing the main feature of the two-nucleon transfer cross sections.

Each final state of $^{26}$Al as the two quasiparticles, however, is not described in a unified way for both ($^3$He, $p$) and ($d$, $\alpha$) reactions. The values used for the probability amplitudes $U_j$ and $V_j$ are the realistic ones obtained from the targets $^{24}$Mg and $^{28}$Si nuclei, respectively.[44,43] The ground states of these two target nuclei have different properties,[54] which can be understood by such a term as "deformation" in the Nilsson model. The agreement obtained in this analysis, therefore, only implies that the present model can explain separately the two-nucleon transfer strengths for the low-lying states of $^{26}$Al in their relation to the target ground states.

## V. DISCUSSION AND CONCLUSIONS

It was shown that the two-nucleon transfer strengths to the low-lying states of $^{26}$Al were consistent with the idea that the $K=0$ and $K=5$ bands have opposite signs of the deformation parameter to the other $K=1$, $K=2$, and $K=3$ bands in the framework of the Nilsson model with pairing correlation (model 1). On the other hand, the simple pairing model of the spherical nucleus (model 2) predicted well the overall features of the two-nucleon transfer strengths for the low-lying states of $^{26}$Al for both ($d$, $\alpha$) and ($^3$He, $p$) reactions, although this success was attained by assuming that the final states of $^{26}$Al were described separately for the stripping to $^{24}$Mg and the pick-up from $^{28}$Si.

The correspondence between the two models employed in the present analysis is not obvious theoretically. However, the two-quasiparticle configurations in model 2 correspond generally to the dominant components of the shell-model basis of the two-Nilsson-quasiparticle configurations in model 1. For example, the ground-state configuration $(\frac{5}{2}[202])^2$ in model 1 consists of only one shell-model component $(d_{5/2})^2$, which is the configuration in model 2. This ground state configuration has a two-hole character for $\beta < 0$ and a two-particle character for $\beta \geq 0.1$, because the energy of the $\frac{5}{2}[202]$ orbital changes

steeply with change of the deformation and because it is much lower than the Fermi surface for $\beta<0$ and higher than that for $\beta\geq 0.1$ (see Fig. 6). These two phenomena are probably related to the character of the $^{26}$Al nucleus, which will be discussed in the following paragraphs. The configuration $(\frac{1}{2}[211])^2$ of the $K=1$ band head assumed for the 1.850-MeV $1^+$ state in model 1 has a two-particle character with a dominant shell-model component of $(s_{1/2})$.[2] This shell-model basis is the configuration in model 1.

It should be remembered that in model 2, realistic values of the occupation numbers were used for the target ground states for each reaction. This procedure implies that model 2 is not the simplest model on a spherical basis, and some correlation is introduced implicitly through the occupation numbers of the target ground state employed in the calculations. Furthermore, these values were different between $^{24}$Mg and $^{28}$Si. This fact and the well-known nature of the direct reaction—that the target ground state is retained in the final states as the spectator cores—brought the two different cores into description of the low-lying states of $^{26}$Al. This supports the idea that these states are characterized by the coexistence of such different cores, as can be represented by different deformations in model 1.

The coexistence of states with different natures has been widely observed in the periodic table.[55-58] Recently, the projected Hartree-Fock method was applied[27] to $^{27}$Al and $^{27}$Si, which are also located in the transition region of the $1s$-$0d$ shell. The interplay between the prolate and oblate Hartree-Fock states was important in these nuclei.

The features of $^{26}$Al found in the present study can be observed only under the following circumstances: (1) when the two-nucleon transfer reactions excite preferentially the states that have strong two-particle correlation, and (2) when $^{26}$Al is situated in the transition region where an increase of four mass units results in a complete change of shapes of nuclei.

## ACKNOWLEDGMENTS

The authors are indebted to Prof. Y. Shida and Prof. T. Udagawa for their valuable discussions. They thank Dr. M. Igarashi for helping them in DWBA calculations and Dr. Y. Tanaka for permitting them to use his computer code for calculating the pairing Nilsson wave functions. Their deep gratitude is due to Prof. Y. Nogami, Prof. A. Arima, and Prof. H. Kamitsubo for their encouragement during the present work. The assistance and hospitablity of the staff in the Low-Energy Physics Division of the Institute for Nuclear Study are also greatly appreciated.

---

*Present address: Cyclotron Institute, Texas A & M University, College Station, Texas 77843.
†Present address: Kernfysisch Versneller Instituut, Rijksuniversiteit Groningen, The Netherlands.
‡Present address: Kitazato University, Sagamihara-shi, Kanagawa, Japan.
§Present address: Indiana University Cyclotron Facility, Milo B, Sampson Lane, Bloomington, Indiana 47401.
||Present address: Department of Physics, Faculty of Science, Kyushu University, Fukuoka, Japan.
¶Present address: Institute for Physical and Chemical Research, Wako-shi, Saitama, Japan.

[1]P. M. Endt and C. van der Leun, Nucl. Phys. A310, 1 (1978); A214, 1 (1973); A248, 153 (1975).
[2]C. E. Moss, C. Detraz, and C. S. Zaidins, Nucl. Phys. A174, 408 (1974).
[3]P. Horvat, P. Kump, and B. Povh, Nucl. Phys. 45, 341 (1963).
[4]O. Hausser and N. Anyas-Weiss, Can. J. Phys. 46, 2809 (1968).
[5]C. M. Da Silva and J. C. Lisle, Nucl. Phys. A116, 452 (1968).
[6]G. A. Bissinger, P. A. Quin, and P. R. Chagnon, Nucl. Phys. A115, 33 (1968).
[7]G. A. Bissinger, P. A. Quin, and P. R. Chagnon, Nucl. Phys. A132, 529 (1969).
[8]G. A. Bissinger and C. R. Gould, Part. Nucl. 3, 105 (1972).
[9]J. F. Sharpey-Schafer, D. C. Bailey, P. E. Carr, A. N. James, P. J. Nolan, and D. W. Viggars, Phys. Rev. Lett. 27, 1463 (1971).
[10]H. G. Price, A. N. James, P. J. Nolan, J. F. Sharpey-Schafer, P. J. Twin, and D. A. Viggars, Phys. Rev. C 6, 494 (1972).
[11]H. G. Price, P. A. Butler, A. N. James, P. J. Nolan, and J. F. Sharpey-Schafer, Phys. Rev. C 10, 415 (1974).
[12]C. R. Gould, D. R. Tilley, and N. R. Roberson, Phys. Rev. C 7, 1068 (1973).
[13]E. O. De Neijs, M. A. Meyer, J. P. L. Reinecke, and D. Reitmann, Nucl. Phys. A230, 390 (1974).
[14]A. Weidinger, R. H. Siemssen, G. C. Morrison, and B. Zeidman, Nucl. Phys. A108, 547 (1968).
[15]R. R. Betts, H. T. Fortune, and D. J. Pullen, Nucl. Phys. A299, 412 (1978).
[16]H. Fuchs, K. Grabisch, P. Kraaz, and G. Röschert, Nucl. Phys. A110, 65 (1968).
[17]R. R. Betts, H. T. Fortune, and D. J. Pullen, Phys. Rev. C 6, 957 (1972).
[18]B. Lawergren and J. Beyea, Phys. Rev. C 6, 2082 (1972).
[19]R. M. Del Vecchio, R. T. Kouzes, and R. Sherr, Nucl. Phys. A265, 220 (1976).
[20]E. Rivet, R. H. Pehl, J. Cerny, and B. G. Harvey,

Phys. Rev. 141, 1021 (1966).
[21]J. Kroon, B. Hird, and G. C. Ball, Nucl. Phys. A204, 609 (1973).
[22]D. L. Show, B. H. Wildenthal, J. A. Nolen, Jr., and E. Kashy, Nucl. Phys. A263, 293 (1976).
[23]R. R. Betts, H. T. Fortune, and D. J. Pullen, Phys. Rev. C 8, 670 (1973).
[24]R. Jahr, K. Kayser, A. Kostka, and J. P. Wurm, Nucl. Phys. 76, 79 (1966).
[25]C. P. Browne, Phys. Rev. 114, 807 (1959).
[26]P. Wasielewski and F. B. Malik, Nucl. Phys. A160, 113 (1971).
[27]F. Brut and S. Jang, Phys. Lett. 77B, 355 (1978).
[28]Y. Hirao, T. Tanabe, M. Sekiguchi, K. Sato, M. Fujita, T. Yamazaki, Y. Sakurada, T. Honma, N. Yamazaki, M. Furuya, T. Yamada, and H. Ogawa, in *Proceedings of the Seventh International Conference on Cyclotrons and Their Applications* (Birkhauser, Basel, 1975), p. 103.
[29]Y. Hirao, T. Tanabe, M. Sekiguchi, K. Sato, M. Fujita, T. Yamazaki, Y. Sakurada, T. Honma, N. Yamazaki, M. Furuya, T. Yamada, and H. Ogawa, in *Proceedings of the Seventh International Conference on Cyclotrons and Their Applications* (Birkhauser, Basel, 1975), p. 312.
[30]The thickness of this target was estimated by comparing the $\alpha$-particle yield of the ground-state transition of the $(d,\alpha)$ reaction from this target with that from another target with a known thickness.
[31]S. Kato, T. Hasegawa, and M. Tanaka, Nucl. Instrum. Methods 154, 19 (1978).
[32]T. Hasegawa, M. Tanaka, S. Kato, H. Yokomizo, K. Iwatani, H. Hasai, and F. Nishiyama, INS Annual Report 1976, p. 11.
[33]S. Kikuchi, I. Nonaka, H. Ikeda, H. Kumagai, Y. Saji, J. Sanada, S. Suwa, A. Isoya, I. Hayashi, K. Matsuda, H. Yamaguchi, T. Mikumo, K. Nishimura, T. Karasawa, S. Kobayashi, K. Kikuchi, S. Ito, A. Suzuki, S. Takeuchi, and H. Ogawa, J. Phys. Soc. Jpn. 15, 41 (1960). This cyclotron facility (FF cyclotron facility) was shut down about ten years ago. Although the data analyzed in this paper were taken by using this cyclotron facility, they were not published before.
[34]The thickness of this target was measured in a separate experiment by using a 2.2-MeV proton beam. The angular distribution of the protons elastically scattered from $^{24}$Mg was found to follow the Rutherford scattering. The thickness was estimated by comparing the cross section data of the elastic scattering with the calculated Rutherford cross section.
[35]S. Yoshida, Nucl. Phys. 33, 685 (1962).
[36]N. K. Glendenning, Phys. Rev. 137, B102 (1965).
[37]I. S. Towner and J. C. Hardy, Adv. Phys. 18, 401 (1970).
[38]R. A. Broglia, C. Riedel, and T. Udagawa, Nucl. Phys. A135, 561 (1969).
[39]A. Bohr and B. R. Mottelson, K. Dan. Vidensk. Selsk. Mat-Fys. Medd. 27, No. 16 (1953).
[40]J. D. Garrett, R. Middleton, D. J. Pullen, S. A. Andersen, O. Nathan, and Ole Hansen, Nucl. Phys. A164, 449 (1971).
[41]J. Bardeen, L. N. Cooper, and J. R. Schrieffer, Phys. Rev. 108, 1175 (1957); N. N. Bogoliubov, Nuovo Cimento 7, 794 (1958); J. G. Valatin, *ibid.* 7, 843 (1958).
[42]S. G. Nilsson, K. Dan. Vidensk. Selsk. Mat-Fys. Medd. 29, No. 16 (1955).
[43]B. H. Wildenthal and J. B. McGrory, Phys. Rev. C 7, 714 (1973).
[44]J. D. Sherman, Ole Hansen, J. R. Powers, and H. T. Fortune, Nucl. Phys. A257, 45 (1976).
[45]M. Toyama and M. Igarashi (private communication).
[46]B. F. Bayman and A. Kallio, Phys. Rev. 156, 1121 (1967).
[47]A. Amusa, Nucl. Phys. A255, 419 (1975).
[48]C. M. Perey and F. G. Perey, At. Data Nucl. Data Tables 17, 1 (1976).
[49]M. Igarashi (private communication).
[50]R. M. Del Vecchio and W. W. Daehnick, Phys. Rev. C 6, 2095 (1972).
[51]H. Nann, B. H. Wildenthal, H. H. Duhm, and H. Hafner, Nucl. Phys. A246, 323 (1975).
[52]M. Guttormsen, T. Pedersen, J. Rekstad, T. England, E. Osnes, and F. Ingebretsen, Nucl. Phys. A338, 141 (1980).
[53]R. R. Betts and H. T. Fortune, Phys. Rev. C. 7, 1257 (1973), and references cited therein.
[54]A. Bohr and B. Mottelson, *Nuclear Structure* (Benjamin, New York, 1975), Vol. 2, and references cited therein.
[55]D. Proetel, R. M. Diamond, P. Kienle, J. R. Leigh, K. H. Maier, and F. S. Stephens, Phys. Rev. Lett. 31, 896 (1973).
[56]J. H. Hamilton, A. V. Ramayya, W. T. Pinkston, R. M. Ronningen, G. Garcia-Bermudez, H. K. Carter, R. L. Robinson, H. J. Kim, and R. O. Sayer, Phys. Rev. Lett. 32, 239 (1974).
[57]J. H. Hamilton, H. L. Crowell, R. L. Robinson, A. V. Ramayya, W. E. Collins, R. M. Ronningen, V. Maruhn-Rezwani, J. A. Maruhn, N. C. Singhal, H. J. Kim, R. O. Sayer, T. Magel, and L. C. Whitlock, Phys. Rev. Lett. 36, 340 (1976).
[58]R. B. Piercey, A. V. Ramayya, R. M. Ronningen, J. H. Hamilton, R. L. Robinson, and H. J. Kim, Phys. Rev. Lett. 37, 496 (1976).